Pergamon

SCIENCE DIRECT

Bioorganic & Medicinal Chemistry 11 (2003) 4263–4274

BIOORGANIC & MEDICINAL CHEMISTRY

Halovirs A–E, New Antiviral Agents from a Marine-Derived Fungus of the Genus *Scytalidium*

David C. Rowley,* Sara Kelly, Christopher A. Kauffman, Paul R. Jensen and William Fenical

Center for Marine Biotechnology and Biomedicine, Scripps Institution of Oceanography, University of California-San Diego, La Jolla, CA 92093-0204, USA

Received 14 February 2003; accepted 5 May 2003

Abstract—Marine micro-organisms represent an under explored resource for the discovery of novel antiviral agents. Here, we describe a series of peptides designated halovirs A–E (**1**–**5**) that are produced during the saline fermentation of a marine-derived fungus of the genus *Scytalidium*. These lipophilic, linear peptides are potent in vitro inhibitors of the herpes simplex viruses 1 and 2. Evidence is presented that the halovirs directly inactivate herpes viruses, a mechanism of action that could be applicable in the prevention of HSV transmission. The total structures of these new compounds were established by a combination of spectral and chemical techniques. Salient structural features of the halovir hexapeptides include a nitrogen terminus acylated by myristic (C14) or lauric (C12) acid, an unusual Aib-Hyp dipeptide segment, and a carboxyl terminus reduced to a primary alcohol. A qualitative analysis of the secondary structures of these molecules using variable temperature NMR experiments and NOE analyses is also reported.
Published by Elsevier Ltd.

Introduction

Since the discovery of penicillin, fungi have been recognized for their ability to produce potentially life saving medicines including the immunosuppressant agent cyclosporine used in organ transplant therapy and the systemic antifungal drug griseofulvin. These compounds were derived from terrestrial fungi which, for decades, have been a productive resource for the discovery of structurally unusual secondary metabolites possessing exciting bioactivities, including antiviral activity.[1] In recent years, however, the productivity of these resources has been in question since the laboratory cultivation of terrestrially derived fungal strains now increasingly results in the isolation of previously studied compounds.

Unlike terrestrial fungi, fungi living in the ocean have not been extensively studied as a source of secondary metabolites. Marine fungi are adapted to a very distinct set of environmental pressures, and there is increasing evidence that these adaptations include the production of unique secondary metabolites.[2] The development of seawater-based isolation and fermentation techniques have recently enabled the discovery of exciting marine fungal metabolites such as the neomangicols, structurally unprecedented halogenated sesterterpenes that possess cytotoxic and antibacterial properties.[3] Other examples include metabolites exhibiting cytotoxic,[4] antiinflammatory,[5] and antifungal[6] activities, as well as inhibitors of viral topoisomerase[7] and protein tyrosine phosphatase[8] enzymes. Clearly, marine fungi represent a frontier resource for the discovery of structurally unique secondary metabolites with anticipated biomedical potential.

As part of a program to define the chemical potential of marine fungi, we recently completed a screening program designed to identify marine microbial metabolites with activity against the herpes simplex virus (HSV). Herpes simplex viruses are well known for their ability to cause a wide variety of infections, to remain latent in their host for life, and to reactivate and cause lesions at or near the initial site of infection.[9] Typical infections include those of oral and genital mucosal tissues, eyes (keratitis), and central nervous system (encephalitis and

*Corresponding author at current address: Department of Biomedical Sciences, College of Pharmacy, University of Rhode Island, 41 Lower College Road, Kingston, RI 02881, USA. Tel.: +1-401-874-9228; fax: 401-874-5048; e-mail: drowley@uri.edu

0968-0896/03/$ - see front matter Published by Elsevier Ltd.
doi:10.1016/S0968-0896(03)00395-X

meningitis). The latter are rare but life-threatening infections, even in immunocompetent hosts. The incidence of HSV-2, the serotype most commonly correlated with genital infection, has risen by 30% in the United States since the late 1970s, and infects one in five Americans above the age of 12.[10] The incidence of HSV-1 associated genital herpes is increasing worldwide,[11,12] and it is becoming clear that herpes lesions facilitate the sexual transmission of other pathogens such as HIV.

Given the above, there is an immediate need for new antiviral drugs to combat HSV in immunocompromised hosts, especially those suffering from AIDS. In these patients, the body's immune capabilities collapse allowing HSV infections to reactivate with serious consequences. The lesions are broader and deeper, and increase the victim's vulnerability to bacterial and fungal superinfections. HSV infections persisting for longer than 1 month are an AIDS defining illness.[13] An aspect of great concern in current HSV chemotherapy is that drug resistant strains are emerging.[14,15] During viral replication in immunocompromised patients undergoing long-term antiviral chemotherapy, strains have evolved that contain genetic mutations making them impervious to current drugs. These emergent strains have caused progressive disease in immunocompromised patients.[16] Obviously, the discovery of new HSV antivirals with novel modes of action is an important goal.

In this paper, we report the discovery of halovirs A–E (**1**–**5**), new marine fungal metabolites with antiviral activity against both HSV-1 and HSV-2. Experimental evidence suggests that these lipophilic, linear peptides directly inactivate the virus, a mode of action that could prove useful for preventing pathogen transmission.

Results

A survey of over 7000 marine microbial extracts identified a marine fungal strain, our isolate CNL240, as a producer of metabolites with significant activity against the herpes simplex virus-1. Strain CNL240 was obtained from a sample of the Caribbean seagrass *Halodule wrightii*. To isolate the fungal strain, a small portion of the seagrass sample was air-dried, cut into small pieces, and placed onto a seawater based agar medium containing the antibiotics penicillin G and streptomycin sulfate to inhibit bacterial growth. After incubation for several days, a small section of fungal hyphae observed growing outward from the plant material was carefully transferred to a secondary isolation plate containing the same agar medium. This process was repeated until a pure culture was obtained as observed by strain morphology and microscopic examination. The fungal strain was identified as a *Scytalidium* sp. by fatty acid methyl ester analysis[17] (FAME, Microbial ID, Inc. Newark, DE, US) with a similarity index of 0.897. Strain CNL240 has been deposited with the American Type Culture Collection in Manassas, VA, USA, and has the ATCC designation 74470.

Nineteen 1-L cultures of strain CNL240 were grown, without shaking, in a seawater-based culture medium. After approximately 20 days, the cultures formed a well developed white mycelium with randomly dispersed, black liquid droplets containing dense spore suspensions. The mycelia were separated from the culture broths by filtration, lyophilized, and extracted with a 1:1 mixture of dichloromethane and methanol. The resulting extract was concentrated in vacuo yielding 375 mg of crude extract per liter. Assay results indicated a strong antiviral effect with an ED_{50} of 10–20 μg/mL against HSV-1 infected Vero cells. HSV-1 testing of an ethyl acetate extract of the cell-free broth indicated that the bioactive materials were present in the mycelium.

Bioassay-guided fractionation of the mycelium extract was pursued first by high-speed countercurrent chromatography using a solvent system composed of 10% hexanes, 30% ethyl acetate, 30% methanol, and 30% water. The upper layer of this biphasic system was used as the mobile phase. The third of five fractions possessed antiviral activity and was further subjected to reversed-phase C-18 flash chromatography using a gradient of 10–0% water in methanol. Subsequent purification of the antiviral fractions by silica gel flash chromatography and C18HPLC afforded halovirs A–E (**1**–**5**) as the major antiviral components (Fig. 1).

Halovir A (**1**) was obtained as a colorless, amorphous solid in 12 mg/L yield. Halovir A analyzed for the molecular formula of $C_{45}H_{83}N_7O_9$ by high resolution FAB mass spectrometry ($[M+Na]^+$ m/z 888.6119; calculated 888.6150) coupled with ^1H and ^{13}C NMR data. The IR spectrum displayed absorptions at 1640 and 1540 cm^{-1} characteristic of amide carbonyl groups, and showed a broad absorption band at 3290 cm^{-1} consistent with the presence of OH and NH functionalities.

Inspection of the ^1H and ^{13}C NMR spectra of **1** in pyridine-d_5 revealed features consistent with a peptide (Table 1). In the ^1H NMR spectrum, resonances typical of amide protons were visible between δ 7–9, and several resonance bands between δ 4–5 were suggestive of amino acid α-hydrogens. A prominent feature of this spectrum was a large, broad peak at δ 1.2 indicative of at least one aliphatic chain. The ^{13}C NMR spectrum displayed seven carbonyl resonances and eight peaks

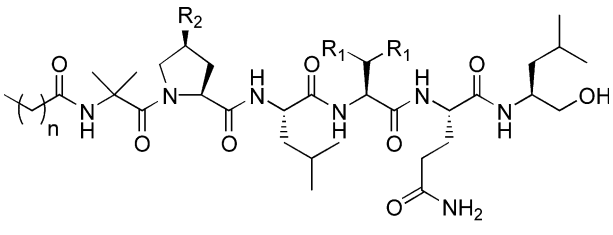

halovir A (**1**) R_1 = Me, R_2 = OH, n = 12
halovir B (**2**) R_1 = H, R_2 = OH, n = 12
halovir C (**3**) R_1 = Me, R_2 = H, n = 12
halovir D (**4**) R_1 = Me, R_2 = OH, n = 10
halovir E (**5**) R_1 = Me, R_2 = H, n = 10

Figure 1. Structures of the halovirs.

between δ 50–70, the region of the spectrum at which α-carbons of peptides normally occur. A region of significantly overlapping peaks was observed near δ 30, and ^{13}C NMR DEPT experiments indicated that all were methylenes. DEPT experiments further revealed that this molecule contained 9 CH_3, 9 CH, and at least one quaternary carbon.

The primary structure of halovir A was deduced by analysis of homo- and heteronuclear 2D NMR data. The amino acids leucine, valine, 4-hydroxyproline, and glutamine, as well as a leucinol (Lol) moiety, were identified by their spin systems observed in TOCSY and COSY NMR experiments and by analysis of NMR chemical shift data. Two methyl groups, both singlets in the ^1H NMR spectrum, were observed to correlate with both a quaternary carbon at δ 57.3 and each other in HMBC NMR experiments, data which established the presence of an α-aminoisobutyric acid residue (Aib). HMBC NMR correlations further verified the other amino acid substructures. ROESY NMR correlations between the γ and ε hydrogens of Gln helped establish its connectivity. The features of a fatty acid derived component were also apparent from these experiments, but the

Table 1. ^1H and ^{13}C Assignments for halovirs A–C (**1**–**3**) in pyridine-d_5

		Halovir A (**1**)		Halovir B (**2**)		Halovir C (**3**)	
		δ ^{13}C[a]	δ ^1H [b]	δ ^{13}C	δ ^1H	δ ^{13}C	δ ^1H
Lol	1	66.0	4.04 (m)	66.0	4.04 (m)	65.9	4.03 (m)
	2	50.8	4.62 (m)	50.9	4.61 (m)	50.7	4.63 (m)
	3	41.2	1.94 (m), 1.76 (m)	41.3	1.95 (m), 1.76 (m)	41.1	1.95 (m), 1.72 (m)
	4	25.6	1.9 (m)	25.6	1.85 (m)	25.5	1.97 (m)
	5	24.3	0.98 (d, 6.3)	24.3	0.99 (d)	24.1	0.99 (d, 6.35)
	6	22.8	0.98 (d, 6.3)	22.7	0.99 (d)	22.7	0.99 (d, 6.35)
	NH		7.76 (d, 9.3)		7.74 (d, 8.7)		7.78 (d, 8.79)
	OH		5.83		5.96		5.87 (bs)
Gln	1	172.8		172.7		172.7	
	2	55.4	5.05 (m)	55.1	5.05 (m)	55.5	5.05 (m)
	3	29.4	2.68 (m)	29.4	2.74 (m)	29.4	2.76 (m)
	4	33.8	2.95 (m)	33.7	2.95 (m)	33.8	2.95 (m)
	5	175.5		175.5		175.4	
	NH_2		8.09 (s), 7.57 (s)		8.08 (s), 7.55 (s)		8.14 (s), 7.62 (s)
	NH		8.12 (d, 7.3)		8.01 (d, 7.8)		8.13 (d, 7.3)
Val/Ala	1	172.8		174.1		172.7	
	2	61.9	4.67 (m)	51.8	4.6 (m)	61.7	4.67 (m)
	3	30.3	2.68 (m)	17.5	1.75 (d, 5.7)	30.0	2.65 (m)
	4	19.6	1.30 (d, 6.8)			19.6	1.28 (d, 6.8)
	5	20.1	1.21 (d, 6.8)			20.0	1.20 (d, 6.8)
	NH		8.12 (d, 7.3)		8.40 (d, 6.3)		8.03 (d, 7.3)
Leu	1	175.8		175.6		175.0	
	2	55.4	4.67 (m)	55.2	4.68 (m)	55.3	4.65 (m)
	3	40.3	2.33 (m), 2.06 (m)	40.0	2.32 (m), 2.04 (m)	40.1	2.33 (m), 2.03 (m)
	4	26.0	2.05 (m)	26.0	2.05 (m)	25.9	2.02 (m)
	5	24.1	1.14 (d, 5.86)	24.0	1.13 (d)	21.5	1.12 (d, 5.4)
	6	21.6	1.02 (d, 5.86)	21.6	1.00 (d)	23.9	1.00 (d, 5.4)
	NH		8.62 (d, 6.35)		8.58 (d, 6.3)		8.50 (d, 6.35)
Hyp/Pro	1	175.4		175.9		175.0	
	2	63.3	5.25 (dd, 9.8, 8.0)	63.6	5.26 (m)	64.4	4.77 (t, 7.3)
	3a	38.4	2.72 (dd, 8.0, 13)	38.4	2.73 (m)	29.7	2.31 (m)
	3b		2.08 (dd, 10, 13)		2.06 (m)		1.80 (m)
	4	70.9	4.75 (m)	71.0	4.77 (m)	26.8	1.80 (m)
	5a	58.2	4.34 (d, 11.2)	58.2	4.33 (m)	49.5	3.58 (m)
	5b		3.81 (dd, 11.2, 2.5)		3.82 (m)		4.02 (m)
	OH		6.99 (d, 2.5)		7.03 (bs)		
Aib	1	175.1		175.4		174.2	
	2	57.3		57.3		57.2	
	3	27.2	1.80 (s)	27.0	1.75 (s)	27.2	1.78 (s)
	4	24.4	1.60 (s)	24.3	1.57 (s)	24.0	1.56 (s)
	NH		9.60 (s)		9.64 (s)		9.62 (s)
Myr	1	174.7		174.8		174.7	
	2	36.3	2.56 (m)	36.2	2.54 (m)	36.2	2.51 (t, 7.3)
	3	26.4	1.77 (m)	26.3	1.80 (m)	26.2	1.77 (m)
	4	32.6	1.25 (m)	32.6	1.24 (m)	32.5	1.25 (m)
	5–12	30	1.2 (m)	30	1.2–1.4 (m)	30.0	1.2 (m)
	13	23.4	1.25 (m)	23.4	1.2 (m)	23.3	1.25 (m)
	14	14.8	0.88 (t)	14.8	0.87 (t)	14.7	0.88 (t)

Assignments by DEPT and HMQC methods.
[a]100 MHz.
[b]300 MHz.

connectivity was quickly lost after C4 due to significant signal overlap in both the ^{1}H and ^{13}C NMR spectra.

The linear peptide of halovir A (**1**) was defined by interpretation of correlations observed in the HMBC and 2D NMR experiments (Table 1). Amide NH and α-protons correlated with their neighboring carbonyl carbons in the HMBC spectrum. Strong sequential $d_{NN}(i,i+1)$ and $d_{\alpha N}(i,i+1)$ NOE signals were present in the ROESY spectrum, further supporting the proposed peptide sequence. ROESY NMR correlations were also observed from the singlet NH of the Aib residue to the δ-proton on the hydroxyproline and both the α- and β-methylenes of the fatty acid moiety. All other HMBC and ROESY NMR correlations observed were consistent with the proposed structure. In consideration of the molecular formula, and by analysis of ^{1}H and ^{13}C NMR data, the terminal acyl group could be assigned as a myristoyl functionality.

The peptide sequence of **1** was further confirmed by the analysis of fragmentation ions produced during electrospray mass spectrometry. Figure 2 shows the dominant product ions generated in an MS^3 experiment. Cleavage across the Aib-Hyp amide bond is the initial dominant fragment. Further collision induced dissociation of the major ion (m/z 569) shows serial loss of the Hyp and Leu residues, each with a molecular weight of 113. MS^3 analysis of the Val-Gln-Lol product ion showed x_1-cleavage across the valine and b_1-dissociation from loss of the Lol. The complete planar structure of halovir A was thus assigned.

Halovir B (**2**) was isolated in a yield of 2 mg/L and found to possess the molecular formula $C_{43}H_{79}N_7O_9$ by high-resolution mass spectrometry (HR-EIMS). Carbon NMR DEPT experiments showed that **2** differed from **1** by having one less methyl group and methine carbon. Analysis of spin systems from TOCSY and COSY NMR data indicated that halovir B contained alanine in place of the valine unit in **1**. Analysis of HMQC, HMBC, and ROESY NMR data, in addition the results from ms/ms experiments, confirmed the presence of alanine and provided the amino acid sequence of **2**.

Halovir C (**3**) was isolated in a yield of 1.5 mg/L and found to possess the molecular formula $C_{45}H_{83}N_7O_8$ by analysis of HR-EIMS and NMR data. The difference in the molecular formula of an oxygen atom from halovir A was attributed to the presence of a proline residue in place of hydroxyproline. The ^{1}H NMR spectrum of **3** lacked the OH signal at ca. δ 7.0 found in **1** and **2**, and the proline β- and γ-methylenes were all appropriately shifted upfield relative to halovirs A and B. Analysis of HMQC, HMBC, ROESY, and DEPT NMR data, in combination with interpretation of ms/ms experiments, were consistent with the presence of proline, and thus the amino acid sequence was assigned for **3**.

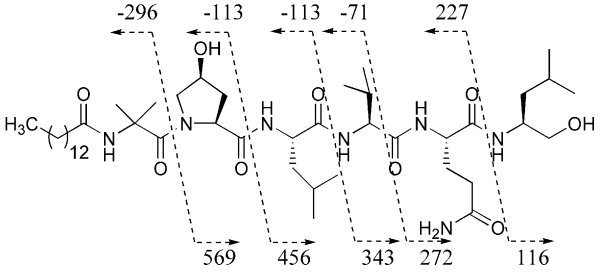

Figure 2. Negative-mode EIMS fragment ions for halovir A (**1**).

During the bioassay-guided fractionation of the antiviral CNL240 extract, chemical analysis of weakly active fractions using C18 electrospray LC–MS led to the discovery of two additional halovir analogues, halovirs D and E (**4**–**5**). The fraction yielding these compounds contained metabolites slightly more polar and with shorter C18HPLC retention times than halovirs A–C. Figure 3 shows the LC–MS chromatogram of this fraction with the y-axis as a function of the total ion current measured in the mass detector. Halovirs D and E (**4**–**5**) were observed by LC–MS on an analytical C18HPLC column using a gradient of 5–100% MeCN (1% CH_3COOH) in H_2O. Preparatory-scale purification was undertaken using C18HPLC leading to the isolation of these lesser abundant analogues. Halovirs D and E analyzed for the molecular formulas $C_{43}H_{79}N_7O_9$ and $C_{43}H_{79}N_7O_8$, respectively, by high-resolution MALDI-FT mass spectrometry coupled with ^{1}H and ^{13}C NMR

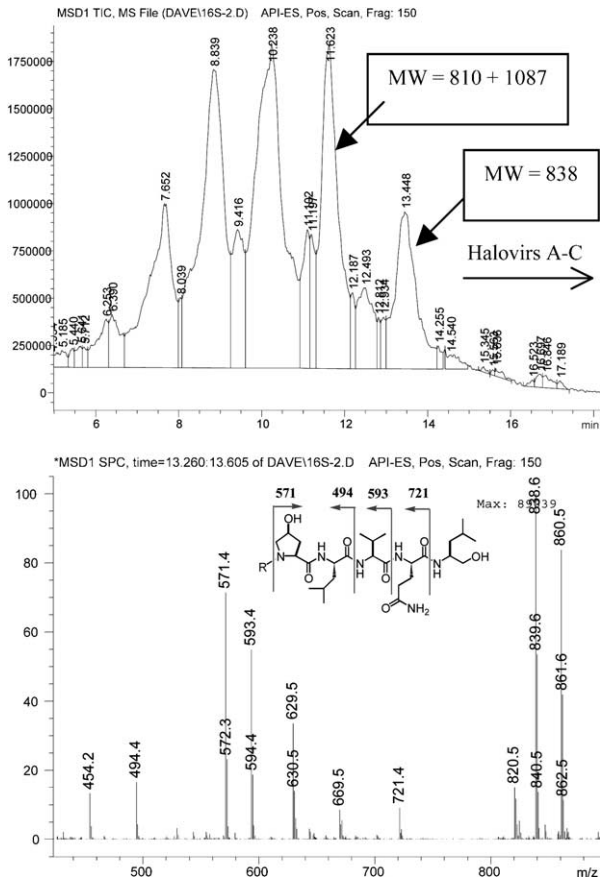

Figure 3. Top: LC–MS chromatogram of a CNL 240 fraction containing the halovirs D and E. The y-axis is the total ion current entering the mass detector. Bottom: mass chromatogram showing molecular and product ion peaks for halovir D (**4**) during the same LC–MS experiment. The 838 and 860 peaks correspond to the $[M+H]^+$ and $[M+Na]^+$ molecular ions, respectively.

data. Analysis of the ^{1}H and ^{13}C NMR spectral data further identified the congeners as containing an Aib residue. Detailed spectroscopic analysis verified that halovirs D and E are analogues of A and C, respectively, but containing a lauric acid acyl moiety on the nitrogen terminus (Fig. 1, Table 2).

The absolute stereochemistry of three of the halovirs were assigned by hydrolysis and analysis of the amino acids by chiral GC–FID methods, and by Mosher's ester NMR analysis. Halovirs A, B, and C were subjected to acid hydrolysis and the amino acids were converted to their isopropyl ester pentafluoropropionamide amino acid derivatives. These derivatives were then characterized by GC–FID on a Chirasil-Val capillary column by comparison and co-injection with identically prepared authentic standards. Using these methods, halovir A was determined to contain L-leucine, L-valine, and L-glutamine. Halovir C additionally contained L-proline. Halovir B was composed of L-alanine, L-leucine, and L-glutamine. In order to determine the stereochemistry of the leucinol (Lol) carboxyl terminus, halovir A was oxidized with Jones reagent to yield the corresponding C-terminal carboxylic acid. Acid hydrolysis, amino acid derivatization, and chiral GC–FID analysis of this derivative showed the presence of only L-leucine, indicating that the original leucinol of halovir A is of the *S* configuration.

Table 2. ^{1}H and ^{13}C assignments for halovirs D–E (**4**, **5**) in DMSO-d_6

		Halovir D (**4**)		Halovir E (**5**)	
		δ ^{13}C[a]	δ ^{1}H[b]	δ ^{13}C	δ ^{1}H
Lol	1	63.8	3.30 (m), 3.16 (m)	63.8	3.28 (m), 3.16 (m)
	2	48.6	3.77 (m)	48.6	3.75 (m)
	3	39.8	1.30 (m)	39.6	1.30 (m)
	4	24.1	1.58 (m)	24.1	1.60 (m)
	5	21.8	0.80 (d)	23.5	0.86 (d)
	6	20.7	0.79 (d)	19.2	0.87 (d)
	NH		7.10 (d, 9.2)		7.11 (d, 8.8)
	OH		4.57 (bt)		4.56 (bs)
Gln	1	170.3		170.3	
	2	52.9	4.09 (m)	52.9	4.07 (m)
	3	27.8	1.80 (m)	27.8	1.78 (m)
	4	31.6	2.05 (m)	31.6	2.05 (m)
	5	173.2		173.3	
	NH_2		7.23 (s), 6.73 (s)		7.21 (s), 6.72 (s)
	NH		7.46 (d, 8.4)		7.45 (d, 7.6)
Val	1	170.1		170.1	
	2	58.8	4.00 (m)	58.6	4.02 (m)
	3	29.4	2.08 (m)	29.5	2.08 (m)
	4	19.1	0.86 (d)	20.6	0.83 (d)
	5	18.3	0.87 (d)	18.3	0.88 (d)
	NH		7.29 (d, 8.4)		7.28 (d, 8.4)
Leu	1	172.5		172.5	
	2	52.5	4.00 (m)	52.6	4.02 (m)
	3	39.0	1.70 (m)	38.3	1.75 (m)
	4	24.5	1.57 (m)	24.6	1.54 (m)
	5	23.5	0.82 (d)	23.2	0.81 (d)
	6	23.1	0.87 (d)	21.8	0.90 (d)
	NH		7.91 (d, 6.8)		7.91 (d, 7.2)
Hyp/Pro	1	172.4		172.4	
	2	61.0	4.38 (dd, 8)	62.4	4.29 (dd, 8)
	3a	36.8	2.13 (m)	28.7	2.20 (m)
	3b		1.60 (m)		1.59 (m)
	4	68.9	4.26 (m)	25.5	1.82 (m)
	5a	56.3	3.71 (m)	48.2	3.75 (m)
	5b		3.23 (m)		3.28 (m)
	OH		5.16 (bs)		
Aib	1	173.1		172.5	
	2	55.6		55.7	
	3	26.0	1.34 (s)	26.1	1.36 (s)
	4	23.5	1.36 (s)	23.4	1.34 (s)
	NH		8.70 (s)		8.71 (s)
Myr	1	172.7		172.8	
	2	34.6	2.20 (m)	34.7	2.20 (m)
	3	24.8	1.48 (m)	24.8	1.51 (m)
	4	31.3	1.22 (m)	31.3	1.22 (m)
	5–10	28.7–29.0	1.22 (m)	28.7–29.0	1.22 (m)
	11	22.1	1.22 (m)	22.1	1.26 (m)
	12	14.0	0.85 (t)	14.0	0.84 (t)

Assignments by DEPT and HMQC methods.
[a]100 MHz.
[b]300 MHz.

The absolute stereochemistry at C-3 of the 3-hydroxyproline residue in halovir A was established by application of the modified Mosher's method (Fig. 4).[18] The Hyp secondary hydroxyl group was esterified with each of the (*S*)- and (*R*)-isomers of 2-methoxy-2-phenyl-2-(trifluoromethyl)acetic acid chlorides (MTPACl). Analysis of the proton NMR signals from both the (*S*)- and (*R*)-MTPA esters allowed $\Delta\delta$ values to be calculated ($\Delta\delta = \delta_S - \delta_R$). Analysis of the $\Delta\delta$ values established the Hyp-C3 absolute stereochemistry to be in the *R* configuration. This determination, coupled with the finding of L-proline in halovir C, shows that the hydroxyproline residues of halovirs A and B possess the L-4-*trans*-configuration.

Secondary structure of halovir A

Peptide molecules often adopt regular secondary structures in solution that are intimately associated with their biological properties. These polypeptide conformations are stabilized through the formation of hydrogen bonds between amide proton and carbonyl oxygens in the peptide backbone, leading to such common peptide conformations as α- and 3_{10}-helices and β-sheets. With the halovirs, ^{1}H NMR experiments showed slow deuterium exchange rates for the Lol, Gln, Val, and Leu backbone amide protons in methanol-d_4 and also DMSO-d_6 spiked with D_2O, a property typical of protons involved in hydrogen bonding. The Aib NH, ε-NH_2 of the Gln residue, and both hydroxyl groups all rapidly underwent deuterium exchange under the same experimental conditions. Therefore, a more detailed inspection of the halovir A polypeptide secondary structure was undertaken through further investigation of hydrogen bonding evidence and also by NOE/ROESY observations of short and medium range ^{1}H–^{1}H distances in the peptide backbone.

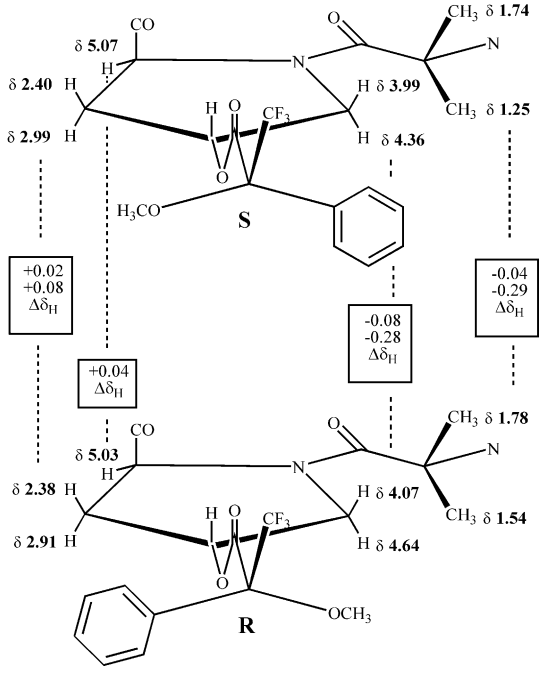

Figure 4. Mosher's ester diagram of (*R*)- and (*S*)-MTPA esters of halovir A. ^{1}H NMR assignments were made in pyridine-d_6 (300 MHz).

The temperature dependence of amide proton chemical shifts are known to correlate with their inaccessibility to solvent, and hence are one indicator of protons potentially involved in hydrogen bonding interactions.[19] It is generally accepted that $\Delta\delta/\Delta T$ coefficients less than 4.0×10^{-3} ppm/K in polar solvents are consistent with amide protons shielded from solvent, while coefficients greater than 5.0×10^{-3} ppm/K are indicative of solvated protons such as those of linear extended peptide conformations.[20] The temperature coefficients for the backbone amide protons of **1** were measured in DMSO-d_6 over a range of 298–388 K (Table 3). The Leu, Val, Gln, and Lol NH protons all clearly satisfy the criteria of having coefficients less than 4.0×10^{-3} ppm/K, indicating inaccessibility to solvent and hence possible participation in intramolecular hydrogen bonding. The middle Val and Leu residues showed the lowest temperature dependence with coefficients of 0.8×10^{-3} and 1.3×10^{-3}, respectively, indicating significant shielding from solvent.

As a second test of hydrogen bonding potential, the solvent dependence of NH chemical shifts was measured as a function of DMSO-d_6 concentration in $CDCl_3$ (Fig. 5).[21] In this experiment, protons with greater exposure to a polar solvent such as dimethyl sulfoxide are better able to participate in intermolecular H-bonding and consequently demonstrate greater chemical shift changes. This effect was observed with the Aib NH, which showed a chemical shift perturbation of nearly 0.75 ppm as the DMSO concentration was increased from 5 to 40%. However, the chemical shifts of the Leu, Val, Gln, and Lol amide protons were practically independent of solvent composition. These data essentially mirror those of the temperature dependence experiment, strongly supporting the participation of the Leu, Val, Gln, and Lol backbone amide protons in hydrogen bonding.

The common secondary structures of polypeptides provide for regular short, medium, and long range ^{1}H–^{1}H

Table 3. Temperature dependence of amide backbone protons of halovir A (**1**)

	Aib	Leu	Val	Gln	Lol
$\Delta\delta/\Delta T$	4.1×10^{-3}	1.3×10^{-3}	0.8×10^{-3}	2.8×10^{-3}	3.1×10^{-3}

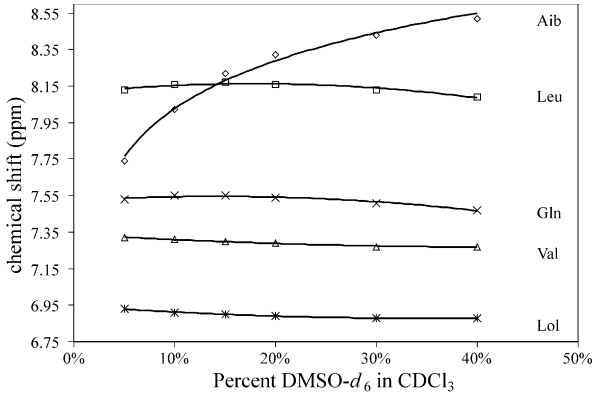

Figure 5. Solvent dependence of NH chemical shifts of halovir A as a function of DMSO-d_6 concentration in $CDCl_3$.

distances that are sufficiently close enough for observation by NOE experiments. Some of these NOEs are suitable for distinguishing between conformations such as α- and 3_{10}-helices and β-sheets.[22] Therefore, the secondary structure of halovir A (**1**) was further investigated by analysis of NOE correlations as measured in a ROESY experiment conducted in DMSO-d_6. Strong sequential $d_{NN}(i,i+1)$ signals were observed in the ROESY spectrum between the Leu, Val, Gln, and Lol residues. Such interresidue correlations are a distinctive feature of polypeptides residing in helical conformations.[22] A complete tracing of successive $d_{NN}(i,i+1)$ correlations through the helical backbone was precluded by the hydroxyproline residue. Dipeptide segments containing proline frequently reside in a *cis*, rather than *trans*, configuration. *Cis–trans* isomerization has a dominant influence on sequential ^1H–^1H distances, with *cis* forms favoring shorter distances between NH_i and $\alpha H_{(i+1)}$, and *trans* configurations providing closer contact between NH_i and $\delta CH_{2(i+1)}$.[23] In the case of the Leu-Hyp dipeptide segment of halovir A, a NOE correlation was observed between the Leu NH and the higher field Hyp δCH, in support of a geometry approaching a *trans*-configuration and a continuing helix through the Leu-Hyp linkage. Looking further down the peptide chain at the Aib-Hyp segment, a strong NOE correlation was observed between the Aib NH and the lower field hydroxyproline δCH_2 (3.68 ppm, DMSO-d_6), indicative of a *trans*-configuration. Taken together, these data are consistent with the hexapeptide segment of halovir A as residing in a helical conformation.

Both α- and 3_{10}-helices are further distinguished from β-sheet formations by close approach of interresidue *i* and $(i+3)$ backbone protons. Other medium-range NOEs are individually characteristic of the two helical types. Short distances prevail between residues *i* and $(i+4)$ in an α-helix, while the more tightly wound 3_{10}-helix is characterized by the close proximity of the *i* and $(i+2)$ amino acid backbone hydrogens.[23] From the Hyp α-H, $d_{\alpha N}(i,i+2)$ and $d_{\alpha N}(i,i+3)$ correlations were observed to the valine and glutamine amide protons, respectively. A NOESY correlation was measured between the leucinol NH and either the Val α-H (i, $i+2$), the Leu α-H (i, $i+3$), or both, but signal overlap precluded distinction between these two. Aib does not contain an α-proton, but weak $d_{\beta N}(i,i+2$ and) $d_{\beta N}(i,i+3)$ correlations were observed between an Aib β-methyl and the leucine and valine NH protons, respectively. A $d_{\alpha\beta}(i,i+3)$ crosspeak was also observed between the Gln α-H and Hyp β-CH_2. These medium-range NOEs are further supportive of a helical solution structure for **1**. Few possible NOE correlations exist to distinguish between α and 3_{10} helices in such a short peptide. However, at least one, and possibly two, $(i,i+2)$ type backbone ^1H–^1H distances lend support in favor of a 3_{10}-helix.

Taken together, the hydrogen bonding evidence and the above NOE data are consistent with halovir A adopting in a 3_{10}-helix. In such a conformation, regular CO_i–NH_{i+3} hydrogen bonds are expected to stabilize the tightly twisted secondary structure. If the myristoyl carbonyl were considered to be CO_i, then in a 3_{10}-helical model it would be involved in a hydrogen bond with the leucine NH. Alternatively, an α-helix is characterized by a series of CO_i–NH_{i+4} hydrogen bonds, and would result in the Myr CO hydrogen bonding with the valine NH. Therefore, an α-helical model of halovir A does not provide a logical hydrogen bonding sequence involving the leucine amide proton.

Figure 6 shows a three-dimensional representation of the peptide portion of halovir A in a 3_{10}-helical configuration. The model was constructed using the standard torsion angles for a 3_{10}-helix. The myristoyl lipophilic chain has been omitted for clarity. It is interesting to note that the model predicts an amphiphilic conformation. The polar primary amide of the Gln and Hyp hydroxyl groups align on one side of the molecule, while the leucine and leucinol lipophilic side chains arrange on the opposite side. Such conformations are common among membrane-active peptides.[24] Of course, while these experiments provide insight into the favored conformations of the halovirs in DMSO, it is conceivable that alternate secondary structures might be preferred in other environments such as aqueous media and lipid bilayers.

Biological properties of the halovir peptides

The halovirs possess potent in vitro activity against herpes simplex virus-1. The antiviral properties were measured in an infectious virus, whole cell assay. Briefly, Vero cells were exposed to virus for 1 h, the infected cells were then treated with compound or control, and the virus-induced cytopathic effects were

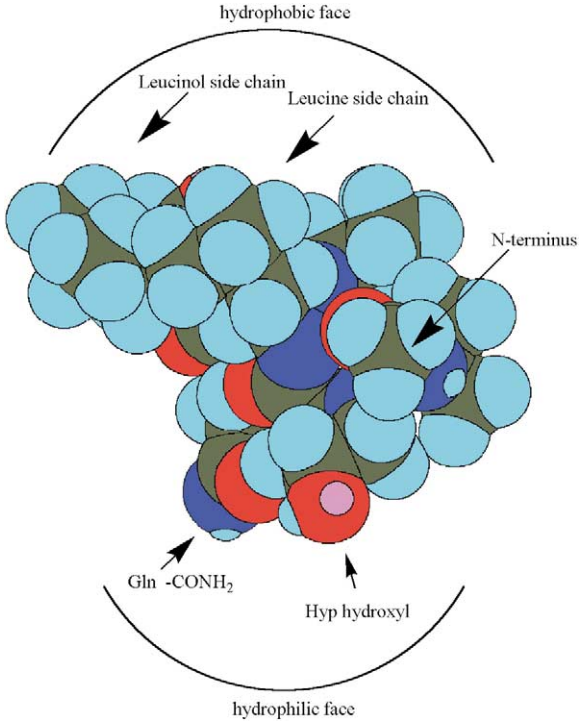

Figure 6. Three-dimensional space-filling model of halovir A in a 3_{10}-helix formation. Twelve carbons of the myristoyl chain have been omitted for clarity. The N-terminus of the peptide backbone appears to extend furthest from the page. Hydrogen atoms appear as light blue, oxygen atoms as red, nitrogen atoms as navy blue, and carbon atoms as gray.

measured after 5 days. Halovirs A, B, and C displayed ED_{50} values of 1.1, 3.5, and 2.2 μM, respectively, when added to cells infected with HSV-1 for 1 h. Halovirs D and E had ED_{50} values of 2.0 and 3.1 μM, respectively, indicating that the length of the lipophilic chain also modulates the antiviral activity.

In addition to inhibiting HSV-1, halovir A was also tested for the inhibition of HSV-2. Halovir A was determined to equally inhibit replication of HSV-1 and HSV-2 with an ED_{50} value of 280 nM in a standard plaque reduction assay (Fig. 7).[25]

Several experiments were performed to provide insight into possible mechanisms involved in the antiviral activities of these peptides. Halovir A (**1**) was studied as a representative compound due to its availability. Two initial assays were designed to determine whether the peptides bind directly to the virus thus inactivating HSV-1. Figure 8 shows the results of pre-incubating infectious HSV-1 with halovir A prior to the addition of virus to Vero cells (Assay #1). A suspension of HSV-1 at 50,000 pfu/mL was exposed to 150 μg/mL of **1** for 2.5 h, then diluted 100-fold and added to Vero cells in microtiter plates (experiment 1). Control experiments included virus in the absence of halovir A (experiment 2), and media with no virus or compound (experiment 3). Additionally, media spiked with halovir A was used to assess compound cytotoxicity at 0.85 μM (experiment 4), and a 'normal assay' was conducted to test for halovir potency on cells pre-infected with virus for one h (experiment 5). The final assay concentration of **1** in all experiments was 0.85 μM, and the assay results were assessed after 5 days of incubation. The experiment demonstrated the virucidal effect of halovir A on HSV-1. Pre-exposing the virus to halovir A resulted in nearly 100% HSV-1 deactivation and complete Vero cell survival. No Vero cell cytotoxicity was observed at 0.85 μM (experiment 4), and this concentration was insufficient to fully protect cells pre-infected with HSV-1 for one h prior to compound addition (experiment 5). Therefore, the antiviral efficacy of halovir A is greater when it is incubated with HSV-1 prior to exposure to Vero cells.

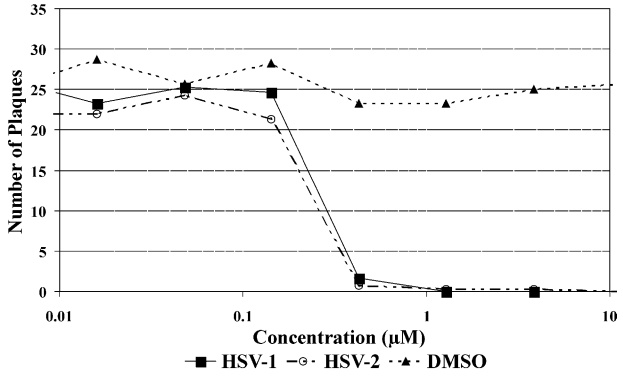

Figure 7. Plaque reduction assay of halovir A against herpes simplex viruses 1 and 2 in Vero cells.

A second assay was designed to explore the concentration and time dependence of the viral inactivation process. In this experiment, viral suspensions consisting of 500 pfu/mL of HSV-1 were added to microtiter plates and treated with serial dilutions of halovir A ranging from 0.08 to 10 μg/mL. The plates were then incubated for 0, 30, and 60 min prior to the addition of virus to the cells. The results were again recorded after 5 days. Figure 9 shows that **1** prevents HSV-1 induced cell lysis in a time dependent manner. ED_{50} values decrease with longer

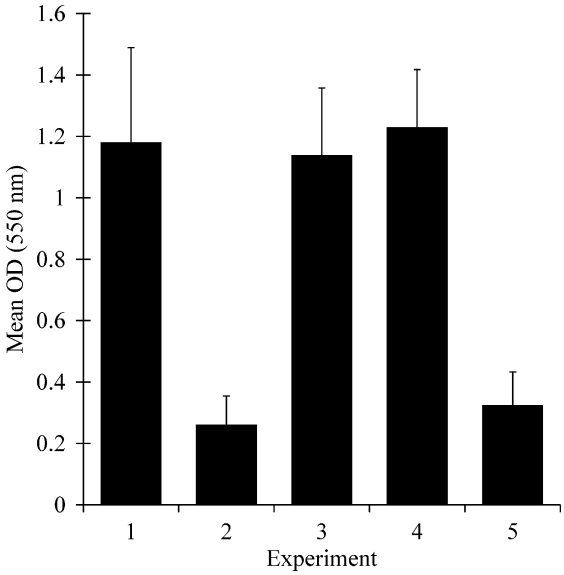

Figure 8. Inactivation of HSV-1 following exposure to halovir A (**1**). In experiment 1, 50,000 pfu/mL HSV-1 were pre-incubated with 150 μg/mL **1** for 2.5 h, diluted 100-fold, added to Vero cells, and incubated for 5 days. The final compound concentration was 0.85 μM. In experiment 2, the virus was treated in a similar manner except without halovir A (DMSO carrier only) and represents normal cell death due to virus. Experiment 3 contained only media with DMSO and represents normal cell survival. In experiment 4, cells were exposed to 0.85 μM halovir A without virus to measure compound cytotoxicity. Experiment 5 represents a standard antiviral assay in which cells are infected with HSV-1 for 1 h prior to treatment with 0.85 μM halovir A.

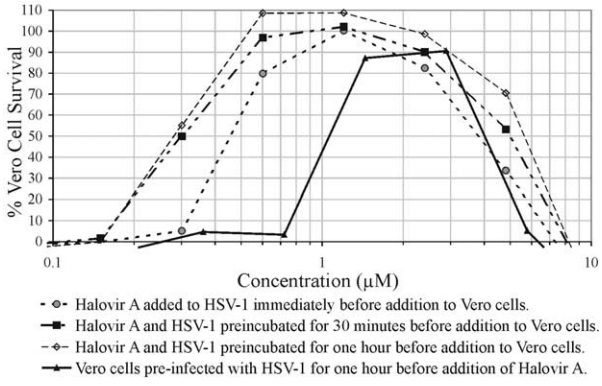

Figure 9. Time and concentration dependent inactivation of HSV-1 by halovir A (**1**). Suspensions of HSV-1 (500 pfu/mL) were treated with serial dilutions of **1**, and then incubated for 0, 30, or 60 min prior to addition to Vero cells. The assay results were recorded after a 5-day incubation. Increased cell protective effects are observed with longer exposures of HSV-1 to halovir A, thus suggesting a virucidal mechanism of action. Compound cytotoxicity effects were also encountered in this assay due to 5-day exposures of Vero cells to **1**.

pre-incubation times, with the maximum effects being reached after 1 h. These results further support a mechanism whereby direct contact of HSV-1 with halovir A results in viral inactivation.

Discussion

A series of linear, lipophilic hexapeptides, designated halovirs A–E, have been isolated from the laboratory cultivation of a marine fungal isolate identified as a *Scytalidium* sp. The halovirs demonstrate activity against both serotypes of the herpes simplex virus in cell-based assays at low and sub-micromolar concentrations. Time and concentration dependent direct inactivation of HSV-1 has been shown, strongly suggesting a virucidal mechanism of action.

Although these are short peptides, hydrogen-bonding evidence, coupled with NOE experiments, suggest a 3_{10}-helical secondary structure leading to an overall amphipathic character. The presence of an Aib residue likely contributes to the helical nature of the halovirs. The additional α-methyl group of Aib restricts the allowed regions of conformational space to those favorable for helices,[26] and Aib has been shown to stabilize 3_{10}- and α-helical peptide conformations.[27] Analysis of Aib-containing peptides of varying lengths indicates that 3_{10}-helices are preferred for peptides with eight or less residues,[27] likely due to the stabilizing effect of the additional hydrogen bond present in the more tightly wound configuration.[28]

Other linear peptides have been reported to directly inactivate the herpes simplex virus, all of which differ from the halovirs by their charged nature. MCP-1 and MCP-2,[29] lysine rich magainins,[30] and synthetic polyhistidine, polylysine, and polyarginine peptides[31] all possess moderate HSV inactivating properties. Myristic and lauric acids also weakly inhibit HSV-1 at concentrations of 16 and 10 mM, respectively.[32] The halovirs are more active by a factor of 10^4 than the free fatty acids. Clearly, the hexapeptide portion is critical to the potent virucidal nature of these molecules, perhaps by intensifying the interaction of the molecules with the viral envelope.

The halovirs share structural similarities with a group of fungal metabolites known as the lipopeptaibols.[33–35] Like other helical, amphiphilic peptides, the lipopeptaibol trichogin A IV displays membrane-modifying properties in a carboxy-fluorescein leakage model.[36] However, the mode of action is unclear since the length of the peptide chain is too short to span a lipid bilayer and form conductance channels. Electron spin resonance[37] and fluorescence quenching experiments[38] have suggested that synthetic analogues of trichogin A IV do not penetrate phospholipid bilayers deeply, but rather orient the peptide portions along the membrane surface. The octanoyl chain is proposed to anchor in the lipid membrane. This orientation is consistent with a 'carpet-like' mechanism of action for membrane destabilization.[38]

The halovirs may interact in an analogous fashion with the lipid envelope of the HSV virus. The infectious HSV virion is encapsulated in a lipid envelope likely acquired from the cytoplasmic membrane of the host cell.[9] The HSV genome codes for 30+ gene products, at least nine of which are eventually incorporated into the virion outer envelope.[9] Membrane destabilization of the viral envelope by halovir A would be consistent with a direct inactivation mechanism. In this instance, the viral particle would be more sensitive to membrane disruptions than host cells.

Membrane destabilization may even be the most effective method for rendering HSV non-infectious. The herpes simplex infection process begins with the attachment of the virus to cell surface receptors, and several viral glycoproteins are likely to be involved. Since HSV must infect at least two very different cell types during its life history, epithelial cells and neurons, it likely has evolved multiple attachment pathways.[9] Therefore, drugs designed to bind to a specific HSV receptor are unlikely to be effective in preventing infection.[39,40]

Aib-Pro dipeptide segments have been proposed to act as molecular hinges in amphiphilic, membrane-modifying peptides such as alamethicin. The Aib-Pro kink may have a dynamic role in facilitating insertion of the peptides into lipid membranes by allowing movement between the N- and C-terminal helical segments.[27] The studies here indicate that the halovir peptides form a continuous helical chain in DMSO. However, other investigations have shown that the exact conformations of short Aib-containing peptides are sensitive to the polarity of their environment.[41] Therefore, alternate conformations of the halovirs are possible, such as in aqueous media or in the presence of a lipid bilayer. Although the Aib-Pro segment could act as a hinge between the fatty acyl chain and the remainder of the peptide portion, it is not immediately apparent why this should be necessary since the saturated hydrocarbon already has inherent flexibility.

More extensive biological evaluation is required to fully assess the potential of the halovirs as antiviral agents. Our experiments demonstrate a pronounced activity against HSV at concentrations that are nontoxic to Vero cells, and it appears likely that the compounds directly inactivate the virus. However, the exact nature of the interaction of these peptides with the virus remains to be clarified. Additional in vitro testing against a range of other viruses, and especially enveloped viruses such as HIV and human cytomegalovirus (HCMV), is warranted to explore the specificity of the observed activity. Also, many in vivo animal models are well established for the evaluation of antiviral agents against herpesvirus infections. A guinea pig or mouse model for HSV vaginitis might be particularly applicable in this case, especially to assess the potential of the halovirs to inhibit sexual transmission. Vaginal microbicides are currently needed in order to help halt transmission of HIV, HSV, and other sexually transmitted diseases.[42]

Experimental

General

Proton and ^{13}C NMR spectra were recorded at 300 and 100 MHz, respectively. NMR spectra were recorded in pyridine-d_5 or DMSO-d_6. DEPT experiments were used to determine the number of attached protons, and all carbon assignments were consistent with DEPT results. HMBC and HMQC experiments were optimized for $^{n}J_{CH}=4$, 6, 8, and 10 Hz and $^{1}J_{CH}=150$ Hz, respectively. ROESY experiments were recorded in DMSO-d_6 and used a mixing time of 300 ms. HPLC separations were accomplished using a Rainin DYNAMAX-60Å C18 column (250×10 mm) at a flow rate of 3 mL/min with refractive index detection. Electrospray ionization mass spectrometry was completed on either a HP 1100 MSD or Finnigan LCQ mass spectrometers.

Bioassay-guided isolation of the halovirs A–E (1–5). The crude mycelial extract (1:1, MeOH–CH_2Cl_2) from a 19-L fermentation was fractionated by high speed counter-current chromatography using a solvent system composed of 10% hexanes, 30% EtOAc, 30% MeOH, and 30% H_2O. The upper layer of the biphasic system was used as the mobile phase. The third of five fractions tested positive for antiviral activity and was further fractionated by reversed-phase silica gel column chromatography using a gradient of 10–0% H_2O in MeOH as the eluant. The fifth of seven fractions was subjected to silica gel column chromatography using a gradient of 5–20% MeOH in CH_2Cl_2. Reversed-phase HPLC (C18 Dynamax) of antiviral fractions 2–4 using 7% H_2O in MeOH yielded pure **1** (231 mg), **2** (41 mg), and **3** (28 mg). The weakly active fourth fraction from the reversed-phase silica gel column chromatography was further purified by gradient C18HPLC (MeOH–H_2O) to yield pure **4** (18 mg) and **5** (7 mg).

Halovir A (**1**) was obtained as a colorless, non-crystalline solid (12 mg/L fermentation yield): HRFABMS $[M+Na]^+$ obsd m/z 888.6119; calcd 888.6150 for $C_{45}H_{83}N_7O_9Na$ (Δ 3.5 ppm); $[\alpha]_D$ −13° (*c* 0.73, MeOH); UV (MeOH) λ_{max}, nm (log ε), 226 (2.58). IR (film) 3284, 2920, 1643, 1537 cm^{-1}. See Table 1 for ^1H and ^{13}C NMR spectral data.

Halovir B (**2**) was obtained as a colorless, non-crystalline solid (2 mg/L fermentation yield): HREIMS $[M+Cs]^+$ obsd m/z 970.4954; calcd 970.4994 for $C_{43}H_{79}N_7O_9Cs$ (Δ 4.1 ppm); $[\alpha]_D$ −8° (*c* 0.25, MeOH), UV (MeOH) λ_{max}, nm (log ε), 225 (3.01). IR (film) 3282, 2928, 1637, 1541 cm^{-1}. See Table 1 for ^1H and ^{13}C NMR spectral data.

Halovir C (**3**) was obtained as a colorless, non-crystalline solid (1.5 mg/L fermentation yield): HREIMS $[M+Cs]^+$ obsd m/z 982.5320; calcd 982.5357 for $C_{45}H_{83}N_7O_8Cs$ (Δ 3.8 ppm); $[\alpha]_D$ −20° (*c* 0.38, MeOH); UV (MeOH) λ_{max}, nm (log ε), 227 (2.90). IR (film) 3282, 2928, 1637, 1536 cm^{-1}. See Table 1 for ^1H and ^{13}C NMR spectral data.

Halovir D (**4**) was obtained as a colorless, non-crystalline solid: MALDI-FTMS $[M+Na]^+$ obsd m/z 860.5828; calcd 860.5831 for $C_{43}H_{79}N_7O_9Na$ (Δ 0.3 ppm); $[\alpha]_D$ −27° (*c* 0.28, MeOH); IR (film) 3281, 2926, 1641, 1542, 1419 cm^{-1}. See Table 2 for ^1H and ^{13}C NMR spectral data.

Halovir E (**5**) was obtained as a colorless, non-crystalline solid: MALDI-FTMS $[M+Na]^+$ obsd m/z 844.5856; calcd 844.5882 for $C_{43}H_{79}N_7O_8Na$ (Δ 3.1 ppm); $[\alpha]_D$ −14° (*c* 0.42, MeOH); IR (film) 3272, 2926, 2855, 1651, 1538 cm^{-1}. See Table 2 for ^1H and ^{13}C NMR spectral data.

Acid hydrolysis of 1–3 and chiral GC analysis. Peptides **1** (5.6 mg), **2** (1.8 mg), and **3** (0.6 mg) were each dissolved in 1 mL of 6 N HCl and heated to 105 °C for 15 h in sealed vials. After solvent evaporation under a stream of N_2 at 105 °C, the crude hydrolysates were treated with isopropyl alcohol (1 mL) and acetyl chloride (250 μL), sealed, and heated to 105 °C for 1 h. The crude products were concentrated under N_2 at 105 °C, cooled to ambient temperature, treated with pentafluoropropionic anhydride (250 μL) in CH_2Cl_2 (1 mL), sealed, and heated to 110 °C for 20 min. The vials were cooled to ambient temperature and concentrated under a stream of N_2. The derivatized hydrolysates were dissolved in CH_2Cl_2 at a concentration of 1 mg/mL, and 100-μL aliquots were injected onto a Chirasil-Val capillary column, which was ramped upwards from 90 °C at 4 °C/min. Elution times were measured by GC–FID and compared to derivatized amino acid standards prepared identically. Halovir A (**1**) was identified as being composed L-leucine, L-valine, and L-glutamine. Halovir B (**2**) included L-alanine in the place of L-valine. Halovir C (**3**) was identified to contain L-proline.

Preparation of carboxylic acid derivative of halovir A, acid hydrolysis, and chiral GC analysis. Halovir A (**1**, 7.9 mg, 9.0 μmol) was dissolved in 2 mL acetone at ambient temperature and treated dropwise with Jones reagent until a brown color persisted for 5 min. A vigorous reaction was initially observed. (Jones reagent was prepared by dissolving 0.67 g of CrO_3 in 19 mL of distilled H_2O and adding 5.8 mL of H_2SO_4 at 0 °C.) The reaction was quenched with 0.5 mL of *i*-PrOH, and then partitioned between 25 mL each of EtOAc and H_2O. The phases were separated and the aqueous phase was further extracted with 2×25 mL of EtOAc. The combined organic phases were dried over Na_2SO_4, filtered, and concentrated in vacuo. The desired compound was purified by C18 reversed-phase HPLC using 10% aqueous MeCN with 0.1% TFA. This synthetic product was more polar than the starting peptide, and a distinctive peak in the ^1H NMR spectrum was observed at 12.3 ppm. The carboxylic acid was subjected to acid hydrolysis, amino acid derivatization, and chiral GC–FID analysis as described above. The hydrolysate was identified as containing only L-leucine by comparison and co-injection with standards.

Preparation of (*R*)-MTPA ester of halovir A (1a). A solution of **1** (8.5 mg, 9.8 μmol) in 500 μL of CH_2Cl_2 was treated with 10 equiv of (*S*)-MTPA chloride (18.3 μL, 98 μmol), diisopropylethylamine (35 μL, 200 μmol),

and a catalytic amount of DMAP. The reaction was stirred at ambient temperature under N_2 for 15 h. The solution was concentrated in vacuo, and the crude product was purified by C18 reversed-phase HPLC using 2.5% H_2O in MeOH to yield 9.6 mg of the ester **1a** (75%). Ester **1a** showed the following spectral characteristics: ^{1}H NMR (300 MHz, pyridine-d_5) 9.70 (s, 1H), 8.61 (d, 6.0, 1H), 8.16 (d, 7.8, 1H), 8.04 (s, 1H), 8.03 (d, 7.2, 1H), 7.92 (d, 7.2, 1H), 7.81 (d, 7.5, 2H), 7.72 (m, 2H), 7.40–7.51 (m, 7H), 5.90 (m, 1H), 5.03 (m, 1H), 5.00 (m, 1H), 4.6–4.8 (m, 6H), 4.03 (dd, 1H), 3.76 (s, 3H), 3.58 (s, 3H), 2.60–2.94 (m, 5H), 2.52 (t, 6, 2H), 2.24–2.42 (m, 2H), 2.06 (m, 2H), 1.7–2.0 (m, 4H), 1.79 (s, 3H), 1.54 (s, 3H), 1.22–1.40 (m, 25H), 1.18 (d, 6.3, 3H), 1.12 (d, 5.1, 3H), 0.98 (d, 5.1, 3H), 0.84–0.92 (m, 9H).

Preparation of (*S*)-MTPA ester of halovir A (1b). Ester **1b** was prepared by the same procedure as described for the preparation of the (*R*)-MTPA ester (**1b**). Ester **1b** showed the following spectral characteristics: ^{1}H NMR (300 MHz, pyridine-d_5) 9.62 (s, 1H), 8.61 (d, 6.3, 1H), 8.09 (d, 7.8, 1H), 8.02 (bs, 1H), 7.93 (d, 7.5, 1H), 7.91 (d, 6.9, 1H), 7.81 (d, 7.8, 2H), 7.67 (m, 2H), 7.36–7.51 (m, 7H), 5.95 (m, 1H), 5.06 (m, 1H), 5.00 (m, 1H), 4.73 (m, 2H), 4.64 (m, 3H), 4.36 (dd, 12.9, 1H), 3.99 (dd, 12.9, 1H), 3.75 (s, 3H), 3.64 (s, 3H), 3.00 (m, 1H), 2.6–2.9 (m, 5H), 2.51 (m, 2H), 2.4 (m, 1H), 2.29 (m, 1H), 1.7–2.1 (m, 6H), 1.74 (s, 3H), 1.22–1.50 (m, 25H), 1.18 (d, 6.7, 3H), 1.13 (d, 5.7, 3H), 1.00 (d, 5.4, 3H), 0.93 (d, 6.0, 3H), 0.91 (d, 6.3, 3H), 0.89 (t, 6.9, 3H).

HSV-1 in vitro antiviral assay. Vero cells were dispensed into 96-well plates at a concentration of 10,000 cells/well in 100 μL of minimum essential medium (MEM) containing 5% fetal bovine serum (FBS). The cells were incubated overnight at 37 °C under 5% CO_2. The media was removed by aspiration, and 100 μL of phosphate buffered saline (PBS) was added to each well and then aspirated. The wells were treated with 100 μL of MEM containing 50 plaque forming units (pfu) of virus and incubated for 1 h (multiplicity of infection = 0.005). Each well was then overlaid with 100 μL of media containing 2% FBS and serial dilutions of any one of the halovirs (A–E) dissolved in DMSO. The compounds were evaluated using a minimum of 10 replicates. After incubation for 5 days, each well was treated with 20 μL of a solution comprising 1.9 mg/mL of MTS (3-(4,5-dimethylthiazol-2-yl)-5-(3-carboxymethoxyphenyl)-2-(4-sulfophenyl)-2H-tetrazolium) and 0.04 mg/mL phenazine methosulfate in phosphate buffered saline (PBS). The cells were incubated for 4 h during which time viable cells metabolize the MTS to a soluble blue formazan. The amount of formazan produced is directly proportional to the number of surviving cells. The optical density of the wells (490 nm) was then assessed using an ELISA plate reader. The plate reader was linked with a computer outfitted with the Softmax® software for data manipulation. A positive growth control (PG), 4 wells/plate, contained non-infected Vero cells grown in the presence of 0.2% DMSO. A viral death control (VD), 4 wells/plate, contained cells infected with HSV-1 and grown in the presence of 0.2% DMSO. Percentage survival was calculated as $(PG-OD_{test})/(PG-VD)*100\%$. Serially diluted acyclovir was used as a standard. Antiviral ED_{50} values were determined by averaging the results from at least 10 replicate assays.

Standardized plaque reduction assays of halovir A (**1**) against HSV-1 and HSV-2 were carried out via contract with MDS Pharma Services. Briefly, compound and virus were added simultaneously to a lawn of Vero cells. Unabsorbed virus and compound were then removed by aspiration after approximately 1 h. The cells were then overlaid with nutrients, and plaque formation was evaluated after several days. Details of the scientific protocol will be available upon request from MDS Pharma Services.

Viral inactivation assay No. 1. Five experiments were performed as follows. *Experiment 1*: HSV-1 at 50,000 pfu/mL and 150 μg/mL halovir A in MEM with 0.6% DMSO. This experiment tests the effects of virus exposure to halovir A prior to cell infection. *Experiment 2*: HSV-1 at 50,000 pfu/mL in MEM with 0.6% DMSO. This is a control to measure cell death due to viral infection in the absence of halovir A. *Experiment 3*: MEM with 0.6% DMSO. This is a control to measure cell survival in the absence of virus and halovir A. *Experiment 4*: Halovir A at 150 μg/mL in MEM with 0.6% DMSO. This is a test for cell cytotoxicity due to halovir A. *Experiment 5*: HSV-1 at 50,000 pfu/mL in MEM with no DMSO. This solution mimics the conditions of the standard in vitro assay where cells are pre-infected with virus in the absence of drug for 1 h. All experimental solutions were vortexed for 30 s and shaken at ambient temperature for 2.5 h. They were vortexed again, and then 100 μL of each was diluted with 9.9 mL of MEM (100× dilution).

Microtiter plates had been prepared with Vero cells overnight, aspirated, washed with PBS, and aspirated again. Cells were then overlaid with 100 μL of one of the five solutions. The plates were incubated at 37 °C under 5% CO_2 for 1 h. At that time, wells containing experiment 1–4 solutions were further overlaid with 100 μL of MEM (2% FBS) and incubated for 5 days. Wells containing experiment 5 were treated with halovir A by adding 100 μL of the solution from experiment 4. The final test concentration of halovir A in each experiment was 0.85 μM. After 5 days incubation, 20 μL of a solution comprising 10 mg/mL of MTT in PBS was added to each well. The plates were incubated for four h, the media carefully aspirated, and then 100 μL of acidified isopropanol was added to each well to dissolve any formazan produced. The acidified isopropanol solution was prepared by adding 50 mL Triton X100 and 2 mL concentrated HCL to 450 mL isopropanol. The optical density of the wells at 490 nm was then assessed using an ELISA plate reader. The results are the average of 80 replicates.

Viral inactivation assay No. 2. In a 96-well microtiter plate, 25 μL aliquots of a HSV-1 suspension (3000 pfu/mL in MEM) were added to 2-fold serial dilutions of **1** prepared in 125 μL of MEM. After incubating at

room temperature for 0, 30, or 60 min, 100 μL of the treated suspensions were transferred to microtiter plates prepared with Vero cells as previously described. After a 1-h incubation at 37 °C under 5% CO_2, the cells were further overlaid with 100 μL of MEM containing 2% FBS. The cells were incubated for 5 days, and then worked-up using the MTS method. The positive growth, viral death, and acyclovir controls were applied to each plate.

Acknowledgements

This research was funded in part by a grant from the National Sea Grant College Program, National Oceanic and Atmospheric Administration, US Department of Commerce, under grant number NA66RGO477 project R-MP-80, through the California Sea Grant College System, and in part by the California State Resources Agency. The views expressed herein are those of the authors and do not necessarily reflect the views of NOAA or any of its sub-agencies. The US government is authorized to reproduce and distribute for governmental purposes. This work was also a result of financial support from the NIH, National Cancer Institute, under grant CA44848.

References and Notes

1. El Sayed, K. A.; In *Studies in Natural Products Chemistry*, Rahman, A., Ed.; Elsevier Science, 2000; Vol. 24, p. 473.
2. Jensen, P. R.; Fenical, W. In *Fungi in Marine Environments*, Hyde, K. D., Ed.; Fungal Diversity: Hong Kong, 2002; Vol. 7, pp. 293–315.
3. Renner, M. K.; Jensen, P. R.; Fenical, W. *J. Org. Chem.* **1998**, *63*, 8346.
4. Toske, S. G.; Jensen, P. R.; Kauffman, C. A.; Fenical, W. *Tetrahedron* **1998**, *54*, 13459.
5. Belofsky, G. N.; Anguera, M.; Jensen, P. R.; Fenical, W.; Kock, M. *Eur. J. Chem.* **2000**, *6*, 1355.
6. Schlingmann, G.; Milne, L.; Williams, D. R.; Carter, G. T. *J. Antibiot.* **1998**, *51*, 303.
7. Hwang, Y.; Rowley, D.; Rhodes, D.; Gertsch, J.; Fenical, W.; Bushman, F. *Mol. Pharmacol.* **1999**, *55*, 1049.
8. Alvi, K. A.; Casey, A.; Nair, B. G. *J. Antibiot.* **1998**, *51*, 515.
9. Roizman, B.; Sears, A. E. In *Fundamental Virology,* 2nd ed., Fields, B. N., Knipe, D. M., Howley, P. M., Eds.; Lippincott-Raven: Philadelphia, 1996; p. 1043.
10. Fleming, D. T.; McQuillan, G. M.; Johnson, R. E.; Nahmias, A. J.; Aral, S. O.; Lee, F. K.; StLouis, M. E. N. *Engl. J. Med.* **1997**, *337*, 1105.
11. Christie, S. N.; McCaughey, C.; McBride, M.; Coyle, P. V. *Int. J. Std. AIDS* **1997**, *8*, 68.
12. Rodgers, C. A.; Omahony, C. *Int. J. Std. AIDS* **1995**, *6*, 144.
13. Wood, M. J. *J. Antimicrob. Chemother.* **1996**, *37*, 97.
14. Field, A. K.; Biron, K. K. *Clin. Microbiol. Rev.* **1994**, *7*, 1.
15. Coen, D. M. In *Antiviral Chemotherapy 4: New Directions for Clinical Application and Research*, Mills, J., Volberding, P., Corey, L., Eds.; Plenum: New York, 1996; p. 49.
16. Erlich, K. S.; Mills, J.; Chatis, P.; Mertz, G. J.; Busch, D. F.; Follansbee, R. M.; Grant, R. M.; Crumpacker, C. S. *N. Engl. J. Med.* **1989**, *320*, 293.
17. Graham, J. H.; Hodge, N. C.; Morton, J. B. *Appl. Environ. Microbiol.* **1995**, *61*, 58.
18. Ohtani, I.; Kusumi, T.; Kashman, Y.; Kakisawa, H. *J. Am. Chem. Soc.* **1991**, *113*, 4092.
19. Stevens, E. S.; Sugawara, N.; Bonora, G. M.; Toniolo, C. *J. Am. Chem. Soc.* **1980**, *102*, 7048.
20. Vervoort, H.; Fenical, W.; Epifanio, R. D. *J. Org. Chem.* **2000**, *65*, 782.
21. Karle, I. L.; Flippen-Anderson, J. L.; Uma, K.; Balaram, H.; Balaram, P. *Biopolymers* **1990**, *29*, 1433.
22. Wüthrich, K.; Billeter, M.and; Braun, W. *J. Mol. Biol.* **1984**, *180*, 715.
23. Wüthrich, K. *NMR of Proteins and Nucleic Acids*; Wiley: New York, 1986.
24. Takahashi, S. *Biochemistry* **1990**, *29*, 6257.
25. Mahy, B. W. J.; Kangro, H. *Virology Methods Manual*; Academic: London, San Diego, 1996.
26. Balaram, P. *Curr. Opin. Struct. Biol.* **1992**, *2*, 845.
27. Sansom, M. S. P. *Q. Rev. Biophys.* **1993**, *26*, 365.
28. Marshall, G. R.; Hodgkin, E. E.; Langs, D. A.; Smith, G. D.; Zabrocki, J.; Leplawy, M. T. *Proc. Nat. Acad. Sci. U.S.A.* **1990**, *87*, 487.
29. Lehrer, R. I.; Daher, K.; Ganz, T.; Selsted, M. E. *J. Virol.* **1985**, *54*, 467.
30. Egal, M.; Conrad, M.; MacDonald, D. L.; Maloy, W. L.; Motley, M.; Genco, C. A. *Int. J. Antimicrob. Agents* **1999**, *13*, 57.
31. Docherty, J. J.; Pollock, J. J. *Antimicrob. Agents Chemother.* **1987**, *31*, 1562.
32. Thormar, H.; Isaacs, C. E.; Brown, H. R.; Barshatzky, M. R.; Pessolano, T. *Antimicrob. Agents Chemother.* **1987**, *31*, 27.
33. Auvin-Guette, C.; Rebuffat, S.; Prigent, Y.; Bodo, B. *J. Am. Chem. Soc.* **1992**, *114*, 2170.
34. Auvin-Guette, C.; Rebuffat, S.; Vuidepot, I.; Massias, M.; Bodo, B. *J. Chem. Soc., Perk. Trans.* **1993**, *1*, 249.
35. Fujita, T.; Wada, S.-I.; Iida, A.; Nishimura, T.; Kanai, M.; Toyama, N. *Chem. Pharm. Bull.* **1994**, *42*, 489.
36. El Hajji, M.; Rebuffat, S.; Le Doan, T.; Klein, G.; Satre, M.; Bodo, B. *Bioch. Biophys. Acta* **1989**, *978*, 97.
37. Monaco, V.; Formaggio, F.; Crisma, M.; Toniolo, C.; Hanson, P.; Millhauser, G. L. *Biopolymers* **1999**, *50*, 239.
38. Epand, R. F.; Epand, R. M.; Monaco, V.; Stoia, S.; Formaggio, F.; Crisma, M.; Toniolo, C. *Eur. J. Biochem.* **1999**, *266*, 1021.
39. Shieh, M. T.; Wudunn, D.; Montgomery, R. I.; Esko, J. D.; Spear, P. G. *J. Cell Biol.* **1992**, *116*, 1273.
40. Wudunn, D.; Spear, P. G. *J. Virol.* **1989**, *63*, 52.
41. Karle, I. L.; Flippen-Anderson, J. L.; Sukumar, M.; Balaram, P. *Int. J. Pept. Prot. Res.* **1988**, *31*, 567.
42. The International Working Group On Vaginal Microbicides. *Aids* **1996**, *10*, 1.